A Comparison of Vibration Behavior of Linear and Nonlinear Bus Driver Seat Suspension System Using the 5DOF Model

Pham Ngoc Dai
Lecturer
Department of Automotive Engineering
Faculty of Transportation Engineering, Ho Chi Minh City University of Technology (HCMUT) – Vietnam National University Ho Chi Minh City, 268 Ly Thuong Kiet Street District 10, Ho Chi Minh City
Vietnam

Vibration of the driver's seat suspension is analyzed using a 5DOF model. The seat's suspension system includes an air spring and hydraulic damper having nonlinear behavior determined experimentally. The random excitation $y_r(t)$ is simulated with ISO 8608 standard through the floor vibration acceleration obtained with the device VM31. Operating parameters include vibration isolation ability SEAT (%), comfort level a_w (m/s^2) (ISO 2631:1-1997), and vibration's effect on health A(8) (2002/44/EC). At an average speed of 48 (km/h), the a_w values of body parts in the linear case are larger than in the nonlinear case, precisely 32%, 40%, 33,5%, and 35,5% in the head, pelvis, upper torso, and lower torso, respectively. SEAT value reaches 93,5% and 74,1% for the linear and nonlinear cases, respectively.

Keywords: *driver seat, nonlinear airspring, nonlinear damper, SEAT, comfort, health*

1. INTRODUCTION

Vibration transmitted from the vehicle to the driver during operation reduces body comfort. Long-term exposure to this vibration can lead to many dangerous occupational diseases [1-3]. The seat suspension systems for drivers of buses, in particular, and road vehicles, in general, have long been researched and applied to reduce the effects of vibration transmitted to the driver [1, 4]. The comfort level and effect on the driver's health as subjected to vibration have long been studied [1, 2]. This influence is related to specific natural frequencies of the body's organs, leading to the response of these organs according to the excitation frequency and amplitude [1, 2]. Similar to the vehicle suspension system with the ability to absorb and dissipate excitation energy transmitted to the vehicle body [5], the seat suspension system has the form of a spring-mass-damper system designed to reduce and dissipate energy over the excitation frequency range before transmitting to the driver [6, 7]. According to simulation and experimental studies, this system has proven effective in isolating vibrations, especially high-frequency ones [6-12].

Using the 1DOF model to simulate the seat suspension system and only considering the excitation from the floor transmitted to the seat, ignoring the influence of the vehicle suspension system and vehicle body, can be mentioned in studies [7-9]. In particular, the study modeled the seat suspension system with an air spring and a nonlinear hydraulic damper tested using excitation signals according to standards for wheel loaders and bulldozers [7]. Research was conducted on applying rotational magnetic damping to the seat suspension system for heavy trucks subjected to harmonic and random excitation [8]. Research the influence of damping parameters on the vibration isolation feature of the seat suspension system with different occupant load modes using the 1DOF model [9]. In addition, experimental studies have also been conducted to evaluate the performance of the seat suspension system [10-12]. In particular, the experimental study compared the effectiveness of vibration isolation and comfort of the bus driver on 03 types of seats with different seat suspension systems subjected to many road conditions and air spring pressure parameters [10]. An experimental study measuring the ability to isolate vibrations of the seat suspension system installed on an agricultural tractor when operating on two types of road surfaces was conducted [11]. The research that evaluated the impact of the seat suspension system on drivers of different ages and genders in two types of buses with different floor height structures was presented [12].

In addition to the 1DOF seat models used in the above studies, the seat suspension models were integrated into the vehicle models [13-19]. Research on the application of the 1DOF driver's seat model integrated into the vehicle 4DOF model for analyzing the driver's vertical and lateral vibration subjected to random excitation [13]. The application of the 2DOF vehicle model integrated a 1DOF seat model and a 5DOF driver model to simulate the driver and seat suspension vertical vibration when subjected to transient excitation [14] and random excitation [15]. The application of a 2DOF vehicle model integrated a 2DOF seat and driver model [16], 2DOF seat, and 4DOF driver model [17], subjected to transient and random excitation. The vehicle model 7DOF application integrated the seat suspension system and driver 5DOF

Received: September 2024, Accepted: February 2025
Correspondence to: Pham Ngoc Dai
Faculty of Transportation Engineering, Ho Chi Minh City University of Technology, Vietnam
E-mail: phamngocdai@hcmut.edu.vn
doi: 10.5937/fme2502196P

model [18] and 1DOF model [19] to evaluate the driver's vertical, longitudinal, and lateral vibration. In addition, research on the application of the 2DOF quarter-vehicle model to analyze the vibration of the vehicle body integrated with the human body has also been proposed [20]. The dynamic behavior model of the air spring used on suspension systems has been studied with an analytical model based on the state change of the air inside the air spring, which can be mentioned [21].

The disadvantage of passive driver seat suspension is that it cannot isolate vibration with low frequencies from 0,5 - 4 (Hz) [7, 9]. When operating on the road, vehicles are stimulated by continuously varied frequency vibration from 0,5 - 20 (Hz) [7]. It is necessary to analyze the seat suspension vibration in specific operating conditions to evaluate the working efficiency of the suspension. However, the assessment of the effect of vibration on the bus driver in Vietnam still needs to be improved. The above studies are still limited in integrating the nonlinearity of elastic, damping elements, and kinematics of guiding elements into a single dynamic model describing the vibration of the occupant. Hence, the evaluation results of the comfort level or vibration isolation efficiency of the system are not optimal. Therefore, this study was conducted to assess the working efficiency of seat suspension and driver behavior when operating vehicles in Vietnam. The seat's suspension system is analyzed specifically with the integration of nonlinear models of the component elements. This study can be applied in designing and optimizing the driver's seat suspension system through the established dynamic analysis model. At the same time, the analysis of the differences between linear and nonlinear models' responses can be used as a basis for selecting the calculation model according to specific cases in practice.

2. EXPERIMENTAL METHOD

2.1 Vehicle floor excitation *y*(*t*)

The vehicle floor's vibration excitation data is collected on the Wenda Gi.34 bus according to the data collection diagram and route on the map in Figure 1. Accordingly, excitation data is collected for specific cases according to working conditions on the actual fixed route of the vehicle from the place of departure (Binh Tan District) to the place of work (Cu Chi Automobile Enterprise). The VM31 device receives acceleration data from the vehicle floor a_{z_floor} (m/s^2) right below the driver's seat position through the KS963B100 sensor in the frequency range 0,2-1500 (Hz) over time in the form of interval root mean square. Compared to the first experiment research [22], the vehicle departed 10 minutes earlier (from 6:20 a.m.) to avoid rush hour congestion in the second experiment. The vehicle arrived at the destination about 50 minutes, 10 minutes earlier than the first experiment [22]. The average vehicle speed reached 48 (km/h) higher than the study [22] 8 (km/h). The average floor acceleration value over the entire time domain is approximately 0,598 (m/s^2), Figure 2.

With the measured floor acceleration signal, research is done to find the optimal reference power spectrum value Φ_{0opt} (m^3/rad) at spatial frequency Ω_0 = 1 (rad/m) according to the instructions of ISO 8608 standard [23], branch 01 of the diagram in Figure 3. The value Φ_{0opt} (m^3/rad) found is continued according to figure 3 in branch 02 to calculate the random excitation signal on the speed domain v [5-80] (km/h), and branch 03 gives the harmonic excitation signal in the frequency domain f [0,5-20] (Hz).

Figure 1. Experimental setup for collecting vehicle's floor excitation data

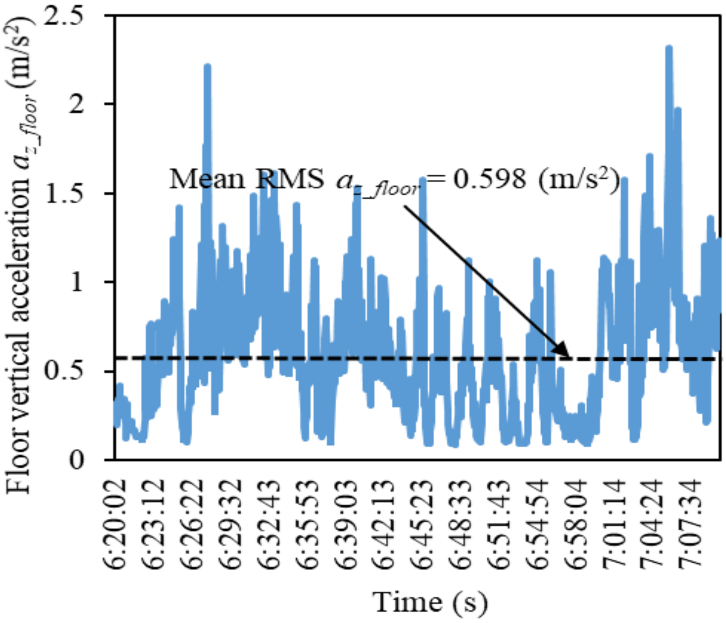

Figure 2. Floor acceleration signal over time a_{z_floor} (m/s²)

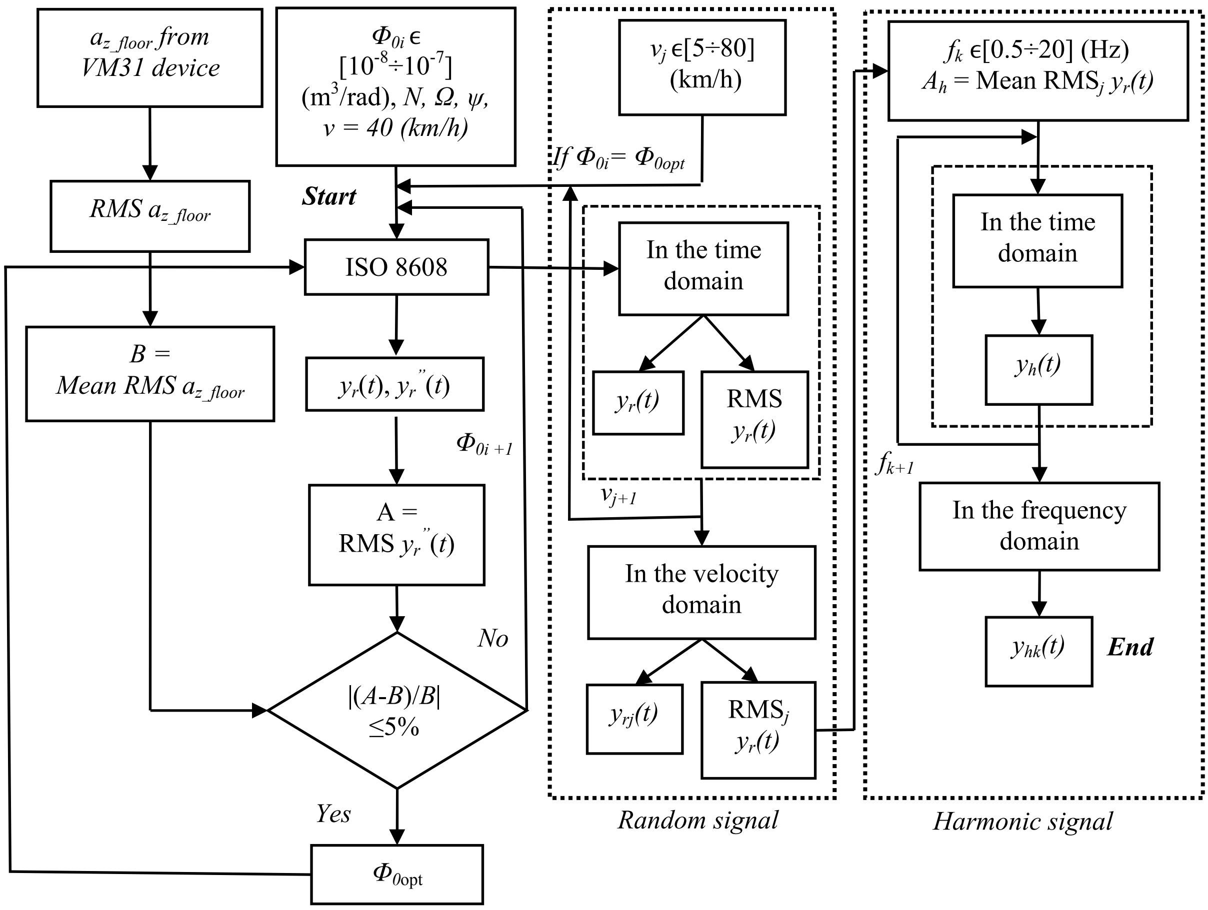

Figure 3. Simulation diagram for random excitation signals in the speed domain and harmonic excitation signals in the frequency domain

2.1.1 Floor excitation random signal $y_r(t)$

The ISO 8608 standard [23] guides the simulation of a random excitation signal over time $y_r(t)$ (m) with the excitation frequency range f [0,5-20] (Hz) [7] and the spectrum value reference Φ_0 (m³/rad) at spatial frequency Ω_0 = 1 (rad/m). The random displacement of the floor surface $y_r(t)$ is calculated according to (1) [17].

$$y_r(t) = \sum_1^N \sqrt{2.\Delta\Omega.\Phi_0.\left(\frac{\Omega_i}{\Omega_0}\right)^{-w}}.\sin\left(\Omega_i.v.t - \psi_i\right) \qquad (1)$$

The equation's components can be describe as: N = 500: The number of sine waves is chosen $i = 1 \div N$: The i^{th} sine wave Ω_i: The wavenumbers Ω_i are chosen to lie at N equal intervals $\Delta\Omega$ (rad/m) (rad/m) v = 48 (km/h): Velocity t: Time (s), ψ_i: the different sets of uniformly distributed phase angles in the range between 0 and 2π (rad), w = 2: The drop in magnitude based on the mathematical model (1) and the implementation diagram in Figure 3, the optimal reference power spectrum value is found to be $\Phi_{0opt} = 3{,}1.10^{-8}$ (m^3/rad), the RMS value of floor acceleration simulation with Φ_{0opt} reaching 0,569 (m/s^2). This value is 4,84% smaller than the measured value of 0,598 (m/s^2).

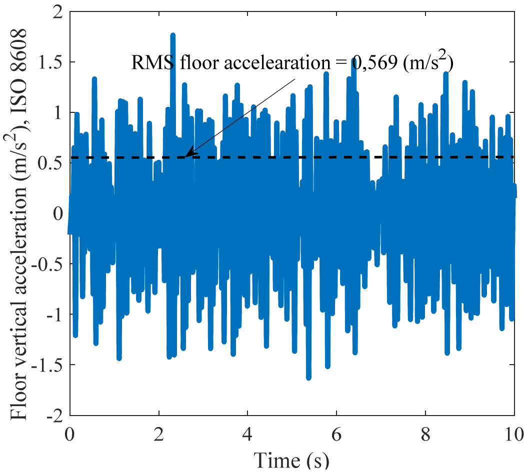

Figure 4. Floor vertical acceleration according to ISO 8608 with $\Phi_{0opt} = 3{,}1.10^{-8}$ (m^3/rad)

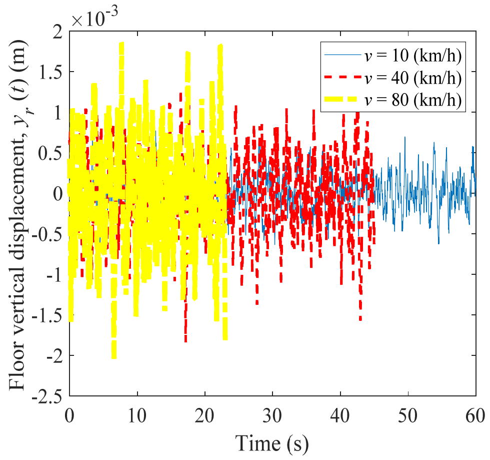

Figure 5. Floor vertical displacement over time $y_r(t)$ (m) at speeds 10 (km/h), 40 (km/h), 80 (km/h)

2.1.2. Floor excitation harmonic signal yh(t)

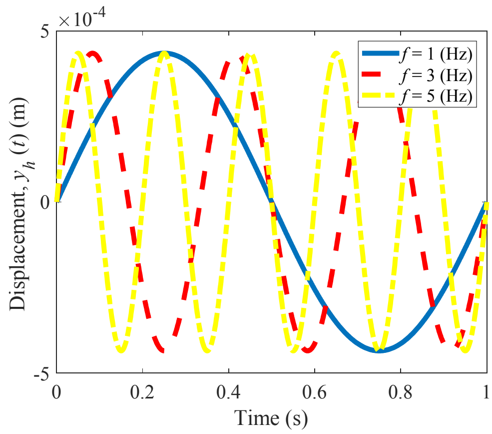

Figure 6. Harmonic excitation

The input excitation $y_h(t)$ has the form of a harmonic function in the vehicle's ordinary working frequency domain f [0,5÷20] (Hz) [7] when moving on the road, according to Figure 6.

The $y_h(t)$ signal in Figure 6 is represented based on equation (2). The amplitude of the harmonic signal $A_h = 4{,}3475.10^{-4}$ (m) is taken based on the average amplitude of random excitation signals in the speed domain, according to Figure 7.

$$y_h\left(t\right) = A_h \sin\left(2\pi ft\right) \text{(m)} \tag{2}$$

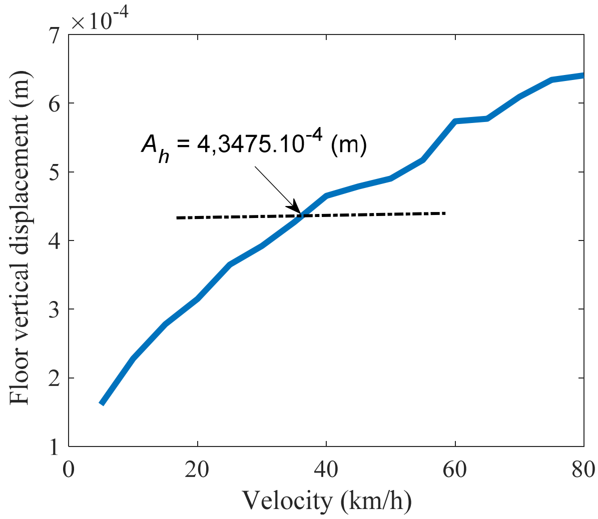

Figure 7. The average amplitude A_h (m) in the velocity domain

2.2 The seat suspension parameters

2.2.1. Air spring's experimental parameters

The air spring reaction force F_{as} (N) according to the deformation y (m) is obtained through the experimental model in Figure 8. Accordingly, the input parameters of the experimental model are the parameters of the air spring on the seat suspension system when the driver is in a balanced position. The total mass placed on the air spring is approximately 100 (kg), initial pressure $P_0 = 1{,}8.10^5$ (N/m^2), air volume $V_0 = 7{,}05.10^{-4}$ (m^3), initial height h_0 = 0,08 (m). The excitation signal is in harmonic form with frequency f = 0,01 (Hz) and amplitude A_x = 0,025 (m). Experimental results of the reaction behavior of the air spring F_{as} (N) corresponding to the deformation y (m) according to Figure 9 and equation (3).

The measurement results in Figure 9 show the nonlinear behavior of the air spring reaction force F_{as} (N) when subjected to expansion and compression. In particular, the change in the magnitude of F_{as} (N) in the compression state is more significant than the expansion state when considering the same magnitude of deformation (compared to the initial equilibrium position). When included in the overall calculation model, the F_{as} value (N) in the same state at any deformation is averaged to simplify the F_{as} reaction parameter (N). The mathematical model describing the average behavior of F_{as} (N) according to y (m) is expressed as (3).

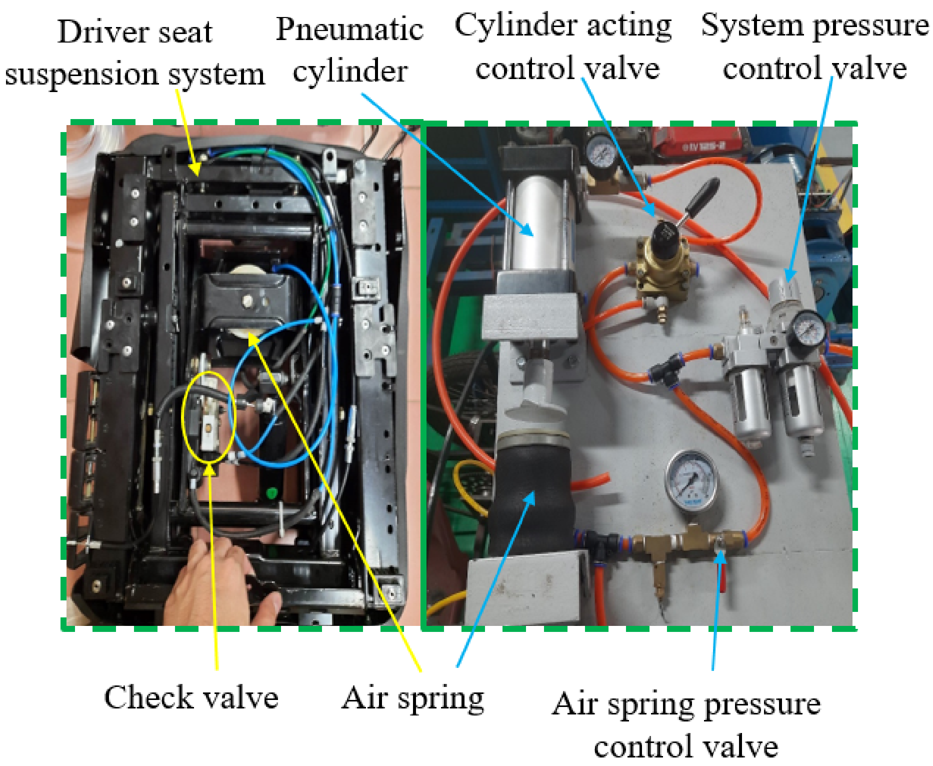

Figure 8. Air spring experimental setup diagram

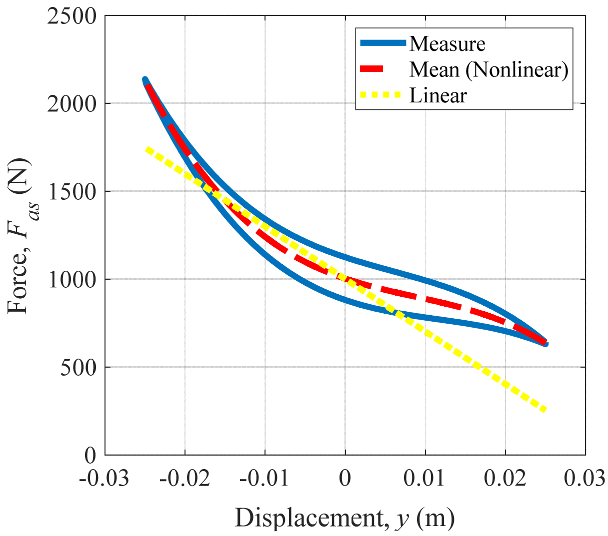

Figure 9. Air spring reaction force F_{as} (N) according to deformation y (m)

Nonlinear

$$F_{as} = -2,3343 \cdot 10^7 \cdot y^3 + 6,0851 \cdot 10^5 \cdot y^2 \ldots -15312 \cdot y + 1002,2 \quad (3)$$

Linear

$$F_{as} = -29880 \cdot y$$

2.2.2 Damper's experimental parameters

The seat suspension damping element installed on the guiding mechanism, figure 8, is the single-tube hydraulic shock absorber. The behavior of the reaction force of the damping element F_d (N) according to the speed dy (m/s) when subjected to excitation is determined with the measurement model of Figure 10. The excitation signal is in harmonic form with frequency f = 3 (Hz), amplitude A_x = 0,02 (m). Experimental results show the behavior of the damping reaction force F_d (N) with speed dy (m/s) in Figure 11. The relationship between damping force F_d (N) and speed dy (m/s) is digitized using the 5th-degree polynomial model according to (4).

Nonlinear

$$F_d = -1,7209 \cdot 10^5 \cdot dy^5 + \ldots - 5201,4 \cdot dy^4 + +30016 dy^3 + 2839,6 \cdot dy^2 + 1336,7 \cdot dy \quad (4)$$

Linear

$$F_d = 2137 \cdot dy$$

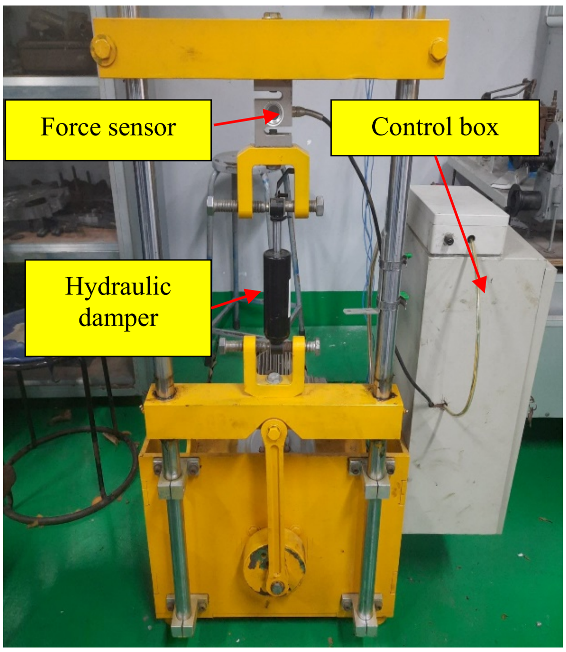

Figure 10. Damper experimental setup diagram

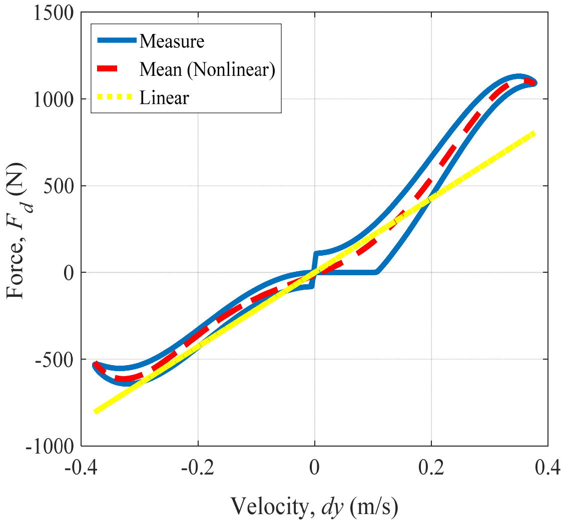

Figure 11. Damper reaction force F_d (N) according to velocity dy (m/s)

3. SIMULATION MODEL

3.1 Driver and seat's suspension system

Model of bus driver's seat suspension system, Figure 12, with an X-shaped guiding mechanism connecting the seat surface at points *B*, *C* and the floor surface at points *A*, *E*. This type of seat suspension system with guiding mechanism only allows to absorb vertical vibrations from the driver. The air spring is permanently connected to the bottom frame and seat frame at points *A* and *B* with bolts. The damping element is installed into the guiding mechanism at the *K* and *L* joints. The driver model is used as a 4DOF bio-dynamic model [24, 25] including parts of the human body such as pelvis, the lower torso, upper torso, and head are connected to each other through elastic and damping joints. Technical specifications of the model are summarized in Nomenclature section.

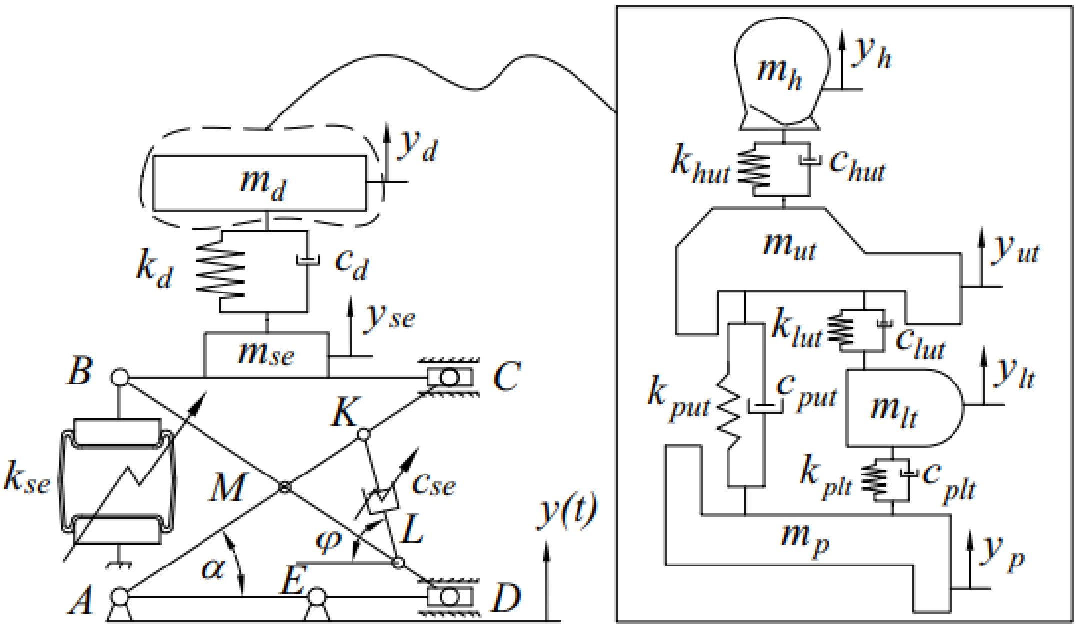

Figure 12. Driver seat dynamic 5DOF model [24, 25]

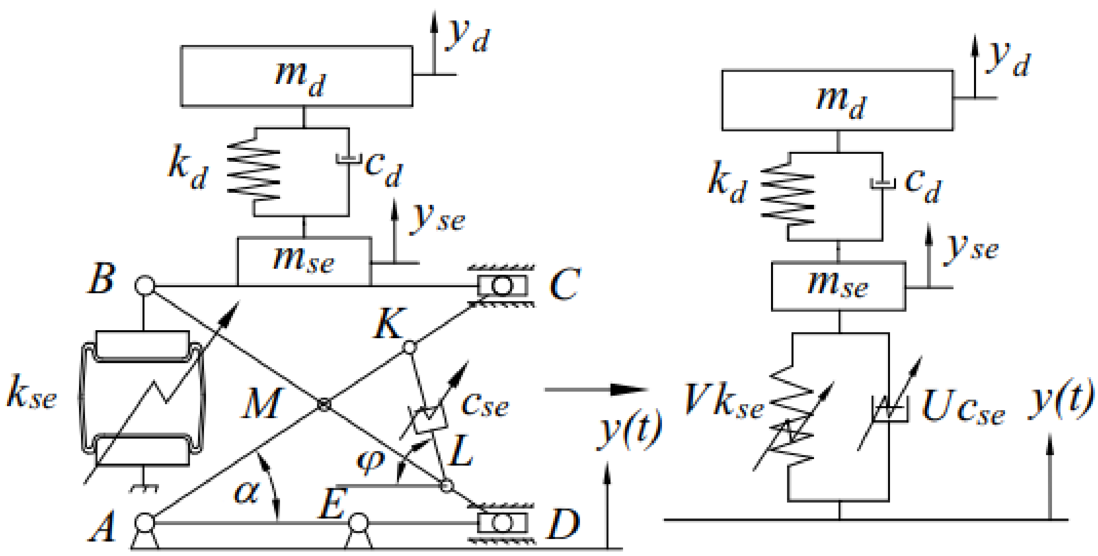

Figure 13. Seat suspension system's equivalent model

3.2 System dynamic equation

3.2.1. Seat suspension – cushion model

The seat suspension system model in Figure 12 with the kinematic influence of the coefficients U and V are obtained from the dynamic analysis of the X-shaped gui–ding mechanism according to the procedure below. The relationship between the rotation angle $\alpha(t)$ (rad) of AC, excitation from the floor surface $y(t)$, and seat surface disp–lacement $y_{se}(t)$ over time is described according to (5), (6).

$$\alpha(t) = \arcsin\frac{l\sin\alpha_0 + y_{se}(t) - y(t)}{l} \text{ (rad)} \tag{5}$$

$$\dot{\alpha}(t) = \frac{\dot{y}_{se}(t) - \dot{y}(t)}{l\cos\alpha} \text{ (rad/s)} \tag{6}$$

The relationship between the rotation angle of dam–per (KL) $\varphi(t)$ according to $\alpha(t)$ is described as (7), (8).

$$\varphi(t) = \arctan\left(\frac{AK - DL}{KC - DL}\tan\alpha\right) \text{ (rad)} \tag{7}$$

Angular velocity:

$$\dot{\varphi}(t) = \dot{\alpha}(AK - DL)(KC - DL)....$$

$$\frac{1}{\cos^2\alpha + \left(\frac{AK - DL}{KC - DL}\sin\alpha\right)^2} \text{ (rad/s)} \tag{8}$$

The relative speed between points K and L in the deformation direction of the damping element KL is analyzed based on the coordinates of points K (x_K, y_K), L (x_L, y_L) according to (9), the speed of point K (v_{xK}, v_{yK}), L (v_{xL}, v_{yL}) according to (10), Figure 14. Assuming the floor is moving upward and the system is expanding, the instantaneous centers of rotation of points K and L are at points A and C, respectively, with corresponding turning radii AK and CL. From the assumption and according to (10), the direction of points K and L velocity vectors is determined according to Figure 14.

$$\begin{cases} x_K = AK\cos\alpha \\ y_K = AK\sin\alpha + y(t) \end{cases}, \begin{cases} x_L = (l - DL)\cos\alpha \\ y_L = DL\sin\alpha + y(t) \end{cases} \tag{9}$$

$$\begin{cases} v_{xK} = -\dot{\alpha}AK\sin\alpha \\ v_{yK} = \dot{\alpha}AK\cos\alpha + \dot{y}(t) \end{cases}, \begin{cases} v_{xL} = \dot{\alpha}(DL - l)\sin\alpha \\ v_{yL} = \dot{\alpha}DL\cos\alpha + \dot{y}(t) \end{cases} \tag{10}$$

From the kinematic model in Figure 14, the relative speed between points K and L in the KL direction is calculated according to (11) when considering the component vectors in the KL direction.

$$v_{KL} = \cos\varphi\left(v_{xK} - v_{xL}\right) + \sin\varphi\left(v_{yK} - v_{yL}\right) \tag{11}$$

Substituting the values from (10) and (11) yields (12).

$$v_{KL} = \dot{\alpha}.\sin\alpha\cos\varphi.\frac{(AK - DL)^2 + (KC - DL)^2}{KC - DL} \tag{12}$$

Separating the joints of the seat suspension system at points A, B, C, D, K, and L and the mass elements, Figure 13, from the system results in a reaction force model, as shown in Figure 15. The friction force between the slider on the slide rails at points C and D is mentioned. The guiding bars of the X-shaped mec–hanism, in reality, have a very small mass (accounting for about 0,6% of the total system mass), so the moment of inertia of these elements is considered negligible.

The force components can be describe as:

F_{Ax}, F_{Ay}, F_{Bx1}, F_{By1}, F_{Bx2}, F_{By2}, F_{Cy1}, F_{Cy2}, F_{Dy}: Reaction force (N) in x and y directions at joints A, B, C and D, respectively

F_{msC1}, F_{msC2}, F_{msD2}: Friction force between slider and sliding rail at joints C, D, respectively

Applying Newton's II law to the force analysis model of Figure 15, the overall mathematical model describing the behavior of mass elements in the system over time is synthesized according to (13), (14).

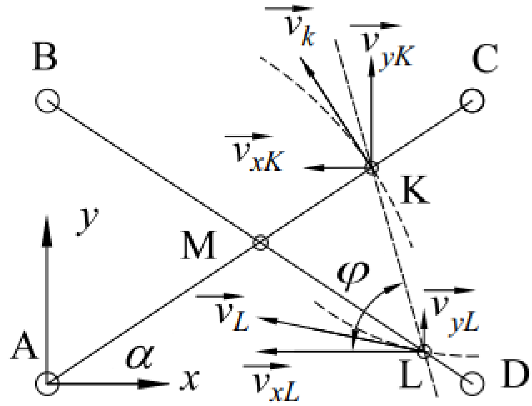

Figure 14. Kinematics of *K* and *L* points

Linear

$$m_{se}\ddot{y}_{se} = Vk_{se}(y_{se} - y) + Uc_{se}(\dot{y}_{se} - \dot{y})...$$
$$+k_d(y_d - y_{se}) + c_d(\dot{y}_d - \dot{y}_{se})$$

$$\begin{cases} V = \dfrac{1}{\mu\tan\alpha - 1} \\ U = \dfrac{2MK.\sin\alpha.\cos\varphi.\sin(\alpha+\varphi)}{(\mu\tan\alpha - 1)(AC\cos\alpha)^2}... \\ \dfrac{\left[(AK - DL)^2 + (KC - DL)^2\right]}{(KC - DL)} \end{cases} \tag{13}$$

Nonlinear

$$m_{se}\ddot{y}_{se} = VF_{as} + UF_d + k_d(y_d - y_{se})...$$
$$+c_d(\dot{y}_d - \dot{y}_{se})$$

$$\begin{cases} V = \dfrac{1}{\mu\tan\alpha - 1} \\ U = \dfrac{2MK\sin(\alpha+\varphi)}{AC\cos\alpha(\mu\tan\alpha - 1)} \end{cases} \tag{14}$$

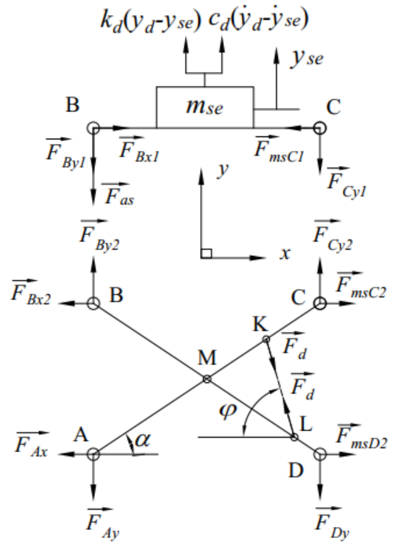

Figure 15. Suspension system's reaction force model

3.2.2 Driver's body model

Separating the mass elements of the driver's body model from the joints results in a reaction model, according to Figure 16. Applying Newton's II law to the force analysis model of Figure 16, the overall mathematical model describing the behavior of the body mass elements over time is compiled according to (15).

4. ASSESSMENT STANDARDS

4.1 Under random excitation

4.1.1 Comfort – ISO 2631:1-1997

The driver's comfort level when affected by whole-body vibrations on the bus is assessed through the overall frequency-weighted acceleration value a_w (m/s^2) according to ISO 2631:1-1997 standard [2]. With a series of instantaneous frequency-weighted acceleration values $a_w(t)$ (m/s^2) during the vibration period from T_1 (s) to T_2 (s), the overall a_w (m/s^2) value is calculated according to (16). W_i is the corresponding weighting filter at frequency f_i in the i^{th} 1/3 octave band, $a_j(t)$ is the j^{th} acceleration value at frequency f_i after the "Fourier" transformation. The comfort level is assessed according to Table 1 based on the obtained a_w value.

Table 1. Driver comfort estimation under different acceleration intensities [2]

Acceleration intensity a_w (m/s^2)	Comfort estimation
a_w < 0,315	Not uncomfortable
0,315< a_w <0,63	A little uncomfortable
0,5< a_w <1	Fairly uncomfortable
0,8< a_w <1,6	Uncomfortable

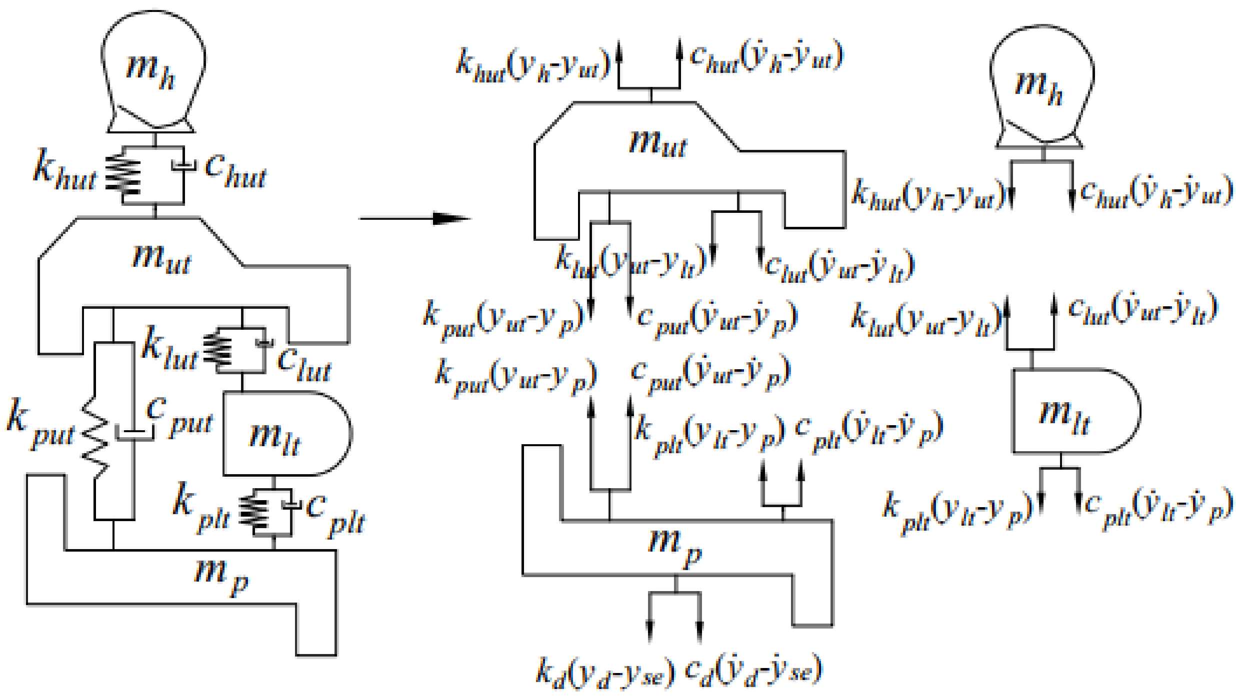

Figure 16. Driver's body free diagram [24,25]

$$\begin{cases} m_p\ddot{y}_p = -k_d\left(y_p - y_{se}\right) - c_d\left(\dot{y}_p - \dot{y}_{se}\right) + k_{put}\left(y_{ut} - y_p\right) + c_{put}\left(\dot{y}_{ut} - \dot{y}_p\right) + k_{plt}\left(y_{lt} - y_p\right) + c_{plt}\left(\dot{y}_{lt} - \dot{y}_p\right) \\ m_{lt}\ddot{y}_{lt} = -k_{plt}\left(y_{lt} - y_p\right) - c_{plt}\left(\dot{y}_{lt} - \dot{y}_p\right) + k_{lut}\left(y_{ut} - y_{lt}\right) + c_{lut}\left(\dot{y}_{ut} - \dot{y}_{lt}\right) \\ m_{ut}\ddot{y}_{ut} = -k_{lut}\left(y_{ut} - y_{lt}\right) - c_{lut}\left(\dot{y}_{ut} - \dot{y}_{lt}\right) - k_{put}\left(y_{ut} - y_p\right) - c_{put}\left(\dot{y}_{ut} - \dot{y}_p\right) + k_{hut}\left(y_h - y_{ut}\right) + c_{hut}\left(\dot{y}_h - \dot{y}_{ut}\right) \\ m_h\ddot{y}_h = -k_{hut}\left(y_h - y_{ut}\right) - c_{hut}\left(\dot{y}_h - \dot{y}_{ut}\right) \end{cases} \tag{15}$$

$$a_w = \sqrt{\frac{1}{T_2 - T_1}\int_{T_1}^{T_2}\left[\sum_i w_i^2\left(\frac{1}{N}\sum_{j=1}^{N} a_j^2(t)\right)\right]dt} \tag{16}$$

Vibrations of the seat suspension system and the driver within the study's limits are only considered in the vertical direction, so the frequency weighting filter w_{kf} is used [2]. Accordingly, the frequency weighting filter value w_{kf} at frequency f (Hz) is determined according to ISO 2631:1-1997 standard [2] (17).

$$w_{kf} = \left|H_h(p)\right|.\left|H_l(p)\right|.\left|H_t(p)\right|.\left|H_s(p)\right| \tag{17}$$

where:

$|H_h(p)|$: High-pass filter (Butterworth characteristics) (18):

$$\left|H_h(p)\right| = \sqrt{\frac{f^4}{f^4 + f_1^4}} \tag{18}$$

$|H_l(p)|$: Low-pass filter (Butterworth characteristics) (19):

$$\left|H_l(p)\right| = \sqrt{\frac{f_2^4}{f^4 + f_2^4}} \tag{19}$$

$|H_t(p)|$: Acceleration-velocity transition filter (20):

$$\left|H_t(p)\right| = \sqrt{\frac{f^2 + f_3^2}{f_3^2}}\sqrt{\frac{f_4^4.Q_4^2}{f^4.Q_4^2 + f^2.f_4^2.\left(1 - 2Q_4^2\right) + f_4^4.Q_4^2}} \tag{20}$$

$|H_s(p)|$: Upward step filter (21):

$$\left|H_s(p)\right| = \frac{Q_6}{Q_5}\sqrt{\frac{f^4.Q_5^2 + f^2.f_5^2.\left(1 - 2Q_5^2\right) + f_5^4.Q_5^2}{f^4.Q_5^2 + f^2.f_5^2.\left(1 - 2Q_5^2\right) + f_6^4.Q_6^2}} \tag{21}$$

4.1.2 Health – 2002/44/EC

According to European standard 2002/44/EC [26], the ability to affect human health when subjected to vibration is assessed based on the value $A(8)$. With the a_w value calculated according to (16) in the period T_1-T_2 (hours), reference time T_0 = 8 (hours), and weighting factor k = 1 (for vertical direction) [26], the value $A(8)$ is calculated according to (22). Human health begins to be affected when the value of $A(8)$ > 0,5 (m/s^2), and if $A(8)$ exceeds 1,5 (m/s^2), health is seriously affected by vibration [26].

$$A(8) = ka_w\sqrt{\frac{T_2 - T_1}{T_0}} \tag{22}$$

4.1.3. Seat effective amplitude transmissibility - *SEAT*

Seat effective amplitude transmissibility - *SEAT* (%) is calculated according to (23). With *SEAT* value > 1, the seat suspension system does not cut down vibrations but amplifies vibrations transmitted to the human body, in contrast to *SEAT* < 1.

$$SEAT = \sqrt{\frac{\int_{T_1}^{T_2} \ddot{y}_{se}^2(t)dt}{\int_{T_1}^{T_2} \ddot{y}^2(t)dt}}.100\,(\%) \tag{23}$$

4.2 Under harmonic excitation

4.2.1 Body acceleration gain response - *GAA$_f$*

The acceleration response of body parts according to frequency (considering the influence of frequency according to ISO 2631 [2]) is investigated through the GAA_f value according to (24). Where, $y_{Seg}''(t)$ (m/s^2) is body's part acceleration over time.

$$GAA_f = \frac{Max\left(\ddot{y}_{Seg}(t)\right)}{\left(2\pi f\right)^2 A_h} w_{kf} \tag{24}$$

4.2.2 Body displacement gain response – *GAD$_f$*

The displacement response of body parts according to frequency is investigated through the GAD_f value (25). Where, $y_{Seg}(t)$ (m/s^2) is body's part displacement over time.

$$GAD_f = \frac{Max\left(y_{Seg}(t)\right)}{A_h} \tag{25}$$

4.2.3 *SEAT$_f$*

Seat effective amplitude transmissibility according to frequency is evaluated by $SEAT_f$ value (26).

$$SEAT_f = \frac{Max\left(\ddot{y}_{Se}(t)\right)}{\left(2\pi f\right)^2 A_h} \tag{26}$$

4.2.4. Suspension relative displacement gain response – *GASRD$_f$*

Suspension relative displacement gain response accor– ding to frequency is evaluated by value $GASRD_f$ (27).

$$GASRD_f = \frac{Max\left|y_{se} - y\right|}{A_h} \tag{27}$$

5. RESULTS AND DISCUSSION

5.1 Random

5.1.1 Time domain

In the average speed mode of 48 (km/h), the acceleration value of human body parts over time is shown in Figures 17, 18, 19, and 20. Acceleration RMS values in the linear case are all over 30% larger than the nonlinear case, specifically 32% in the head, 40% in the pelvis, 33,5% in the upper torso, and 35,5% in the lower torso. Thus, the human body acceleration value in both linear and nonlinear cases results in the level of sensation in range without uncomfortable sensations.

However, the significant difference in acceleration between the two cases needs to be considered for studies with larger stimulation amplitudes to ensure a correct assessment of the actual situation.

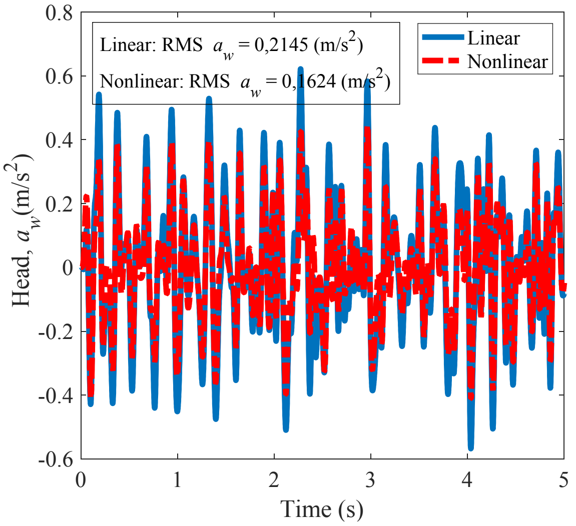

Figure 17. Head's weighted acceleration (m/s^2) in the time domain

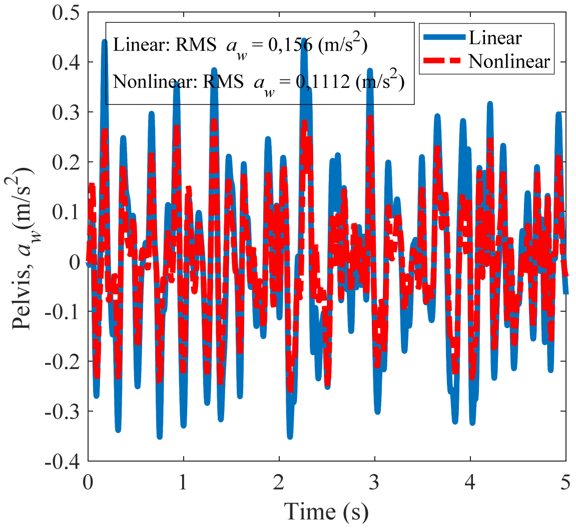

Figure 18. Pelvis's weighted acceleration (m/s^2) in the time domain

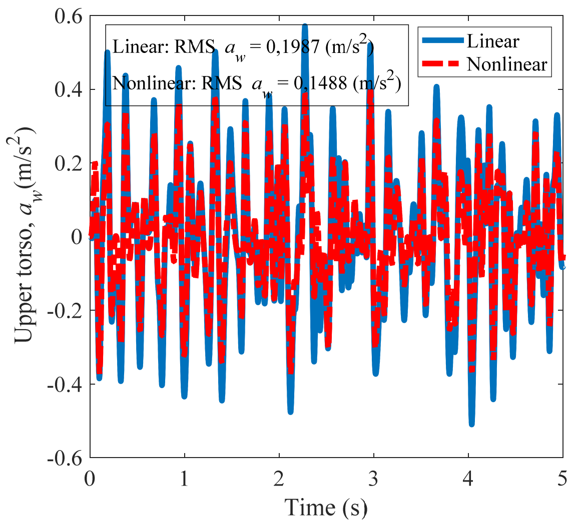

Figure 19. Upper torso's weighted acceleration (m/s^2) in the time domain

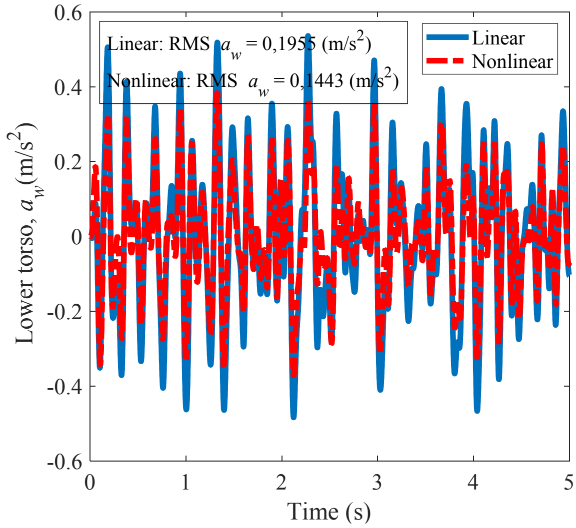

Figure 20. Lower torso's weighted acceleration (m/s^2) in the time domain

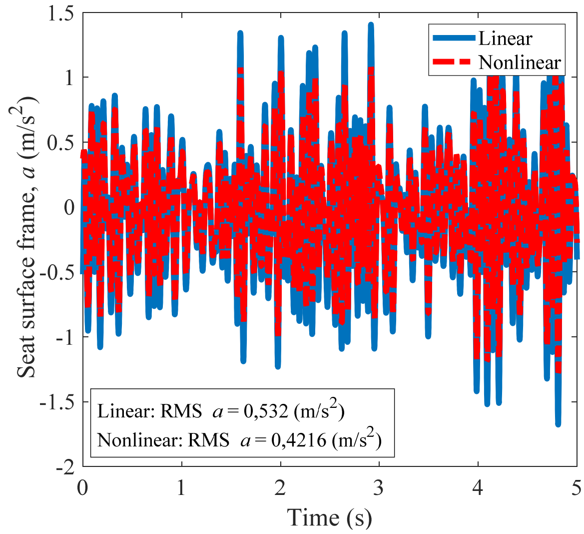

Figure 21. Seat surface frame's weighted acceleration (m/s^2) in the time domain

Besides, when comparing the body's parts, the acce–leration of the head is most significant and gradually decreases, corresponding to the upper torso, lower torso, and pelvis for both linear and nonlinear cases. Specifically, compared to the pelvis, head, upper torso, and lower torso accelerations are 37,5%, 27,4%, and 25,3% larger for the linear case and 46%, 33,8%, and 29,8%, respectively, for the nonlinear case. Accor–dingly, with the human body model chosen [24, 25], the possibility of losing the feeling of comfort increases from the pelvis to the head. From the results of acce–leration values according to ISO 2631:1-1997 [2] of body parts, the value $A(8)$ for health assessment according to standard 2002/44/EC [26] is always guaranteed when the driver only works 50 minutes per day in practice with both linear and nonlinear models. According to Figure 21, the acceleration RMS value in the linear case is 26,2% larger than the nonlinear case for seat frame acceleration. Similarly, the vibration isolation ability of the seat suspension system *SEAT* (%) reaches 93,5% and 74,1% for the linear and nonlinear cases, respectively. Survey cases in the vehicle speed domain in the region 5-80 (km/h) are summarized according to the results below.

5.1.2 Velocity domain

The influence of vehicle speed on the driver's comfort level, health, and the vibration isolation ability of the seat suspension system is surveyed with the results obtained in Figures 22, 23, and 24. Similar to the time domain, the survey values in the speed domain are also compared in both linear and nonlinear cases.

***Comfort**

Figure 22 shows that the comfort level of all parts of the body decreases when the acceleration value according to ISO 2631:1-1997 standard a_w (m/s^2) increases as increasing vehicle speed. However, in all surveyed cases, the driver had a sensation within the range of no discomfort (a_w < 0,315 (m/s^2)). The increase in acceleration with speed of each part is investigated based on the ratio of acceleration at high speeds compared to that at speed 5 (km/h). The calculation results are summarized in Table 2.

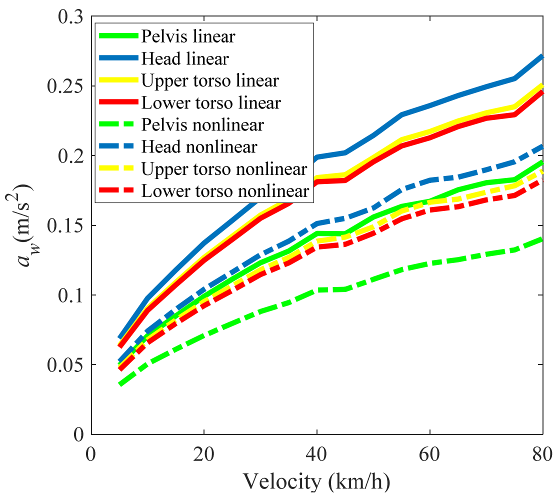

Figure 22. Body segments' RMS weighted acceleration (m/s^2) in the velocity domain

Table 2. The ratio of acceleration at high speeds compared to that at speed 5 (km/h)

Velocity (km/h)	20	40	60	80
Linear				
Pelvis	207,3	301,8	348,7	409,4
Lower torso	199,7	289,9	340,6	393,7
Upper torso	203,1	294,7	359,8	401,6
Head	199,8	289,6	343,3	395,7
Average	202,5	294	348,1	400
Nonlinear				
Pelvis	199,7	291,4	345,2	395,3
Lower torso	199,6	290,4	347,9	394,8
Upper torso	206	299,7	360	408,2
Head	199,6	290,1	353,7	396,3
Average	201,2	292,9	351,7	398,7

Table 2 shows that the level of acceleration increasing of the body's parts according to the speed at each surveyed speed is approximately the same and gradually increases as increasing speed with an average increase of 201% - 202% (20 (km/h)) to 398% - 400% (80 (km/h)) for linear and nonlinear cases, respectively. Accordingly, the average acceleration increase of all parts at each speed of the linear and nonlinear cases has a minimal difference of less than 5%. Considering the same body part, the acceleration in the linear case is always greater than the nonlinear case for all vehicle speed values. In addition, the difference between the linear and nonlinear cases gradually increases with vehicle speed. At a speed of 80 (km/h), the difference in head acceleration is 0,07 (m/s^2), an increase of 2,8 times compared to that at 5 (km/h), which is 0,025 (m/s^2). Similarly, the acceleration in the upper and lower torso is approximately 3.96 times, and the pelvis is 3,34 times.

Considering the same vehicle speed value, similar to the survey results in the time domain, the head acceleration is always the largest, gradually decreasing according to the upper torso, lower torso, and pelvis for both linear and nonlinear cases throughout the speed domain. The acceleration relationship between body parts is evaluated based on the acceleration ratio of the parts compared to the pelvis. The calculation results are summarized in Table 3.

Table 3. The acceleration ratio of the body's parts compared to the pelvis

Velocity (km/h)	20	40	60	80	Average
Linear					
Pelvis	100	100	100	100	100
Lower torso	126	125,7	127,8	125,8	126,3
Upper torso	128	127,8	130,5	128,3	128,7
Head	139	138	141,6	139	139,4
Nonlinear					
Pelvis	100	100	100	100	100
Lower torso	130	129,8	131,2	130	130,3
Upper torso	134,2	133,9	135,8	134,5	134,6
Head	146,6	146,2	148,7	147,2	147,2

Table 3 shows that the acceleration ratio between body parts in the nonlinear case is larger than in the linear case, and this ratio is almost equal at the surveyed vehicle speed values with a slight difference of less than 4%. On average, the acceleration values of the head, upper, and lower torso in the linear case are 39,4%, 28,7%, and 26,3%, respectively, larger than the pelvis and 47,2%, 34,6% and 30,3% in the nonlinear case.

***Health**

The driver acceleration value $A(8)$ is used to evaluate the impact of vibration on health based on the 2002/44/EC standard calculated according to (22) with the actual working time of 50 minutes, resulting in Figure 23. Accordingly, the $A(8)$ value in Figure 23 is calculated according to the acceleration data in Figure 22, so the changing trend of the $A(8)$ value is the same as that of the a_w value. Figure 23 shows that vibration transmitted to the body parts does not affect health in all surveyed cases.

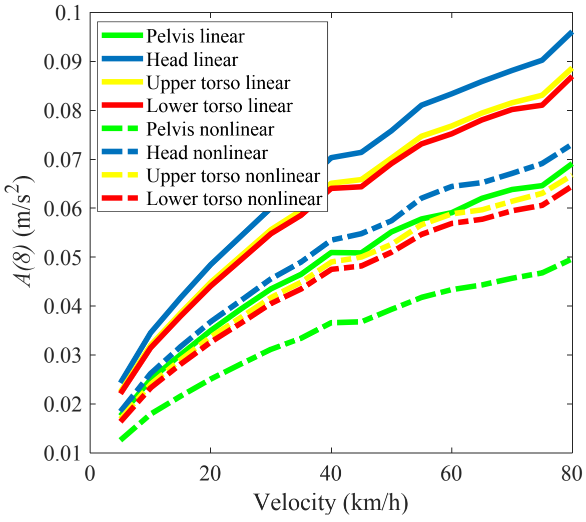

Figure 23. Body segments' $A(8)$ (m/s^2) in the velocity domain

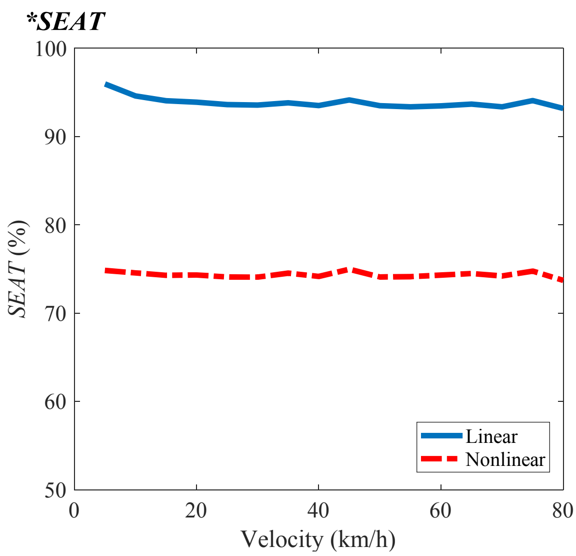

Figure 24. *SEAT* values in the velocity domain

The results in Figure 24 show that the change in *SEAT* value with speed is entirely insignificant. How–ever, the vibration isolation ability of the seat suspen–sion system in the linear and nonlinear cases differs by 19% when the average *SEAT* values in the nonlinear and linear cases are 93% and 74%, respectively. This result shows that the seat suspension system has contributed to reducing from 7% to 26% of vibrations transmitted from the floor to the seat surface when the floor power spectrum has a reference value of Φ_{0opt} = 3,1.10^{-8} (m^3/rad), which is relatively small.

5.2 Harmonic

The acceleration and displacement responses of human body parts and the seat suspension system according to frequency are synthesized and compared for two nonlinear and linear seat suspension systems cases. Accordingly, the difference in the behavior state of the model between the two survey cases at the resonance points (extremes) and behavior change points (starting to exceed 1 and falling below 1) are focused.

5.2.1. Time domain

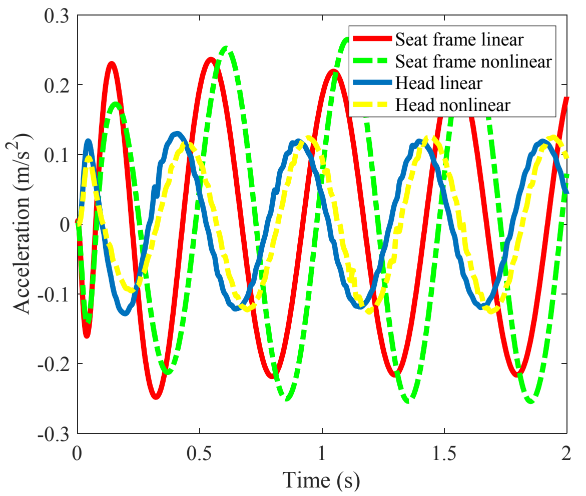

Figure 25. Acceleration response over time at the seat frame and driver's head, with excitation frequency f = 2 (Hz)

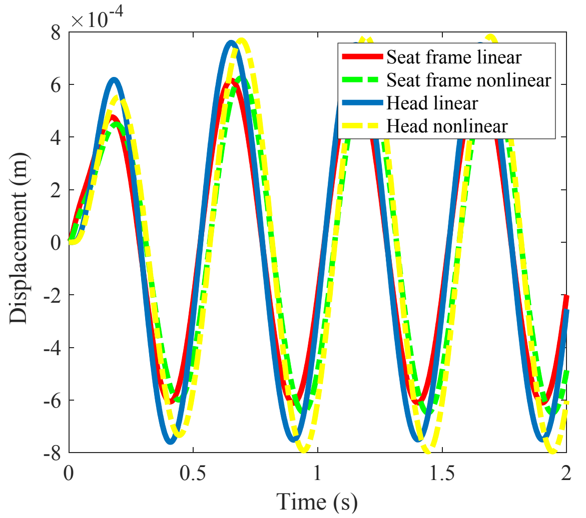

Figure 26. Displacement response over time at the seat frame and driver's head, with excitation frequency f = 2 (Hz)

Figures 25 and 26 depict the response over time at typical elements of the model, such as the seat frame and driver's head, with excitation frequency f = 2 (Hz) for linear and nonlinear seat suspension systems. Accordingly, with the same excitation frequency f at the seat frame, the acceleration response over time of the nonlinear model, when stable, is phase delayed and has an amplitude of 0,26 (m/s^2) higher than that of the linear model 0,215 (m/s^2). However, at the head position, the difference in acceleration amplitude of the two linear and nonlinear cases is minimal, reaching 0,12 (m/s^2), nearly 50% lower than that of the seat frame. The head displacement in Figure 26 is larger than the seat surface displacement in linear and nonlinear cases, corresponding to the acceleration results in Figure 25. In addition, the phase and amplitude differences between the linear and nonlinear cases of the displacement response are minor at steady state.

5.2.2 Frequency domain

Figure 27 shows the acceleration response considering the influence of frequency GAA_f at body parts when subjected to harmonic excitation. In general, the case of a linear suspension system has a more extensive behavior of the frequency and the response values at the resonance point than the case of a nonlinear seat suspension system. Specifically, the resonance point of the linear case is at frequency f = 3,25 (Hz) with value GAA_f = 1,43, and the resonance point of the nonlinear case is at f = 2,5 (Hz), GAA_f = 0,9. Thus, at the reso–nance frequency, the GAA_f value of the linear model is 1,6 times larger than the nonlinear model. In addition, in the nonlinear model, the body parts have approximately the same resonant frequency and response value. In contrast, in the linear model, the resonant frequency of the pelvis is 9,1% lower than the other parts. In the frequency range from 0,5 – 2,5 (Hz), the GAA_f values of the linear and nonlinear cases are equivalent for all body parts. In the frequency range of 2,5 - 8 (Hz), the GAA_f value of the linear case is larger than that of the nonlinear case; outside this frequency range, the acceleration response value between the two cases is approximately the same when considering the same body part. When used, the difference in the gain response and vibration reduction considering the influ–ence of frequency in the two cases should be consi–dered. While in the nonlinear case, the seat suspension system effectively absorbs vibrations throughout the frequency domain, in the linear case, the seat suspension system amplifies vibrations in the frequency range of 2,5 – 5 (Hz).

GAA_f

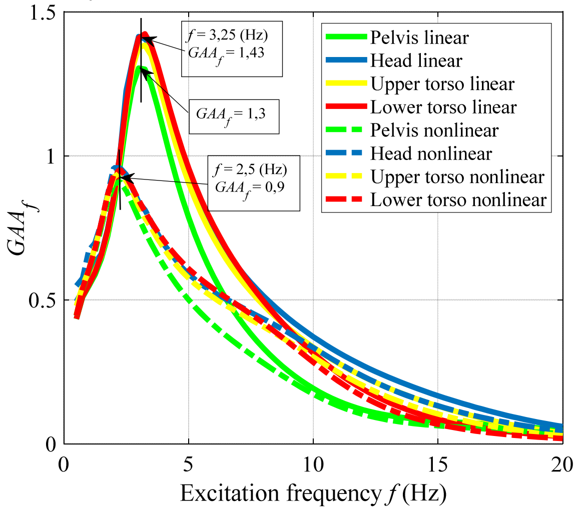

Figure 27. Gain response of the acceleration of the driver's body parts on the frequency domain GAA_f

Figure 28 shows the displacement response of the driver's body parts on the frequency domain GAD_f in linear and nonlinear cases. Similar to the acceleration response in Figure 27, the GAD_f value of the linear case is always higher than the nonlinear case when considering the same body part in the frequency range 2 - 8 (Hz). Outside this frequency range, the GAD_f values of the two cases are approximately the same. The linear case's resonance frequency and response values are 2,75 (Hz) and GAD_f = 2,16, respectively, which are 1,38 times and 1,14 times larger than the resonance frequency, as well as the response values of the nonlinear case. The displacement response of the body parts in both cases exceeded 1, amplified by nearly 90% and 116% in the frequency range 0,5-3,5 (Hz) and 0,5-5 (Hz), corresponding to nonlinear and linear cases.

GAD_f

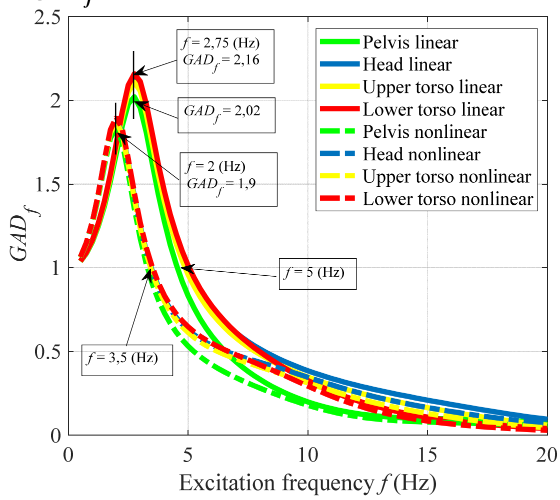

Figure 28. Gain response of the displacement of the driver's body parts on the frequency domain GAD_f

*** $SEAT_f$***

Figure 29 describes the vibration isolation ability of the seat suspension system according to the excitation frequency. Similar to Figure 27 and Figure 28, the $SEAT_f$ value in the frequency range 2 – 8,5 (Hz) in the linear case is always higher than in the nonlinear case and is approximately the same outside the above frequency range. In addition, in the frequency range 0,5 – 8,5 (Hz), the $SEAT_f$ value is always higher than 1, so the vibrations from the floor transmitted to the driver's body are amplified by the highest amount of 285% and 345%, respectively with nonlinear and linear cases. In the frequency range greater than 8,5 (Hz), the $SEAT_f$ value is always less than 1, so the seat suspension system isolates vibrations at high frequencies well. The amplification of vibrations in the low resonant frequency region of 1,5 - 5 (Hz) and the effective isolation of vibrations in the higher frequency region are consistent with the results of studies [6,7,9]. Thus, the maximum $SEAT_f$ value of the linear case is 16% larger than the nonlinear case, corresponding to $SEAT_f$ = 4,45 at f = 3 (Hz) and $SEAT_f$ = 3,85 at f = 2 (Hz).

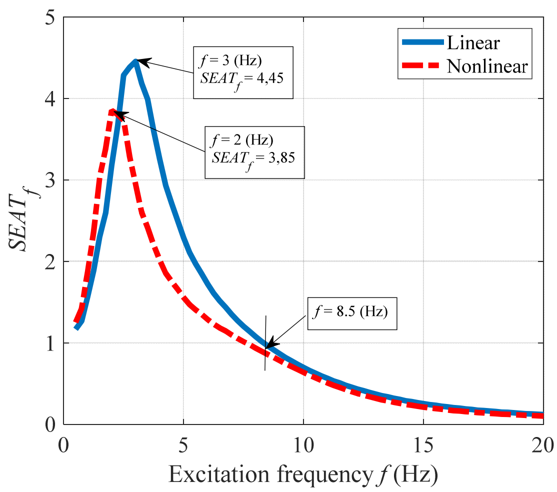

Figure 29. Seat effective amplitude transmissibility in the frequency domain $SEAT_f$

* $GASRD_f$

Considering the excitation frequency domain, the relative displacement response value of the seat suspension system compared to the excitation from the floor $GASRD_f$ only exceeds 1 in the frequency range of 1,9 – 4,5 (Hz). The highest level of displacement ampli–fication ranges from 22% at frequency f = 3,25 (Hz) to 30% at frequency f = 2,5 (Hz) for linear and nonlinear cases, respectively. In the frequency range from 0,5 – 2,5 (Hz) and 4,5 - 20 (Hz), the $GASRD_f$ value in the nonlinear case is always larger than the linear case. In addition, in the frequency range from 0,5 – 2,5 (Hz) and 9,5 - 20 (Hz), the $GASRD_f$ value increases as increasing excitation frequency.

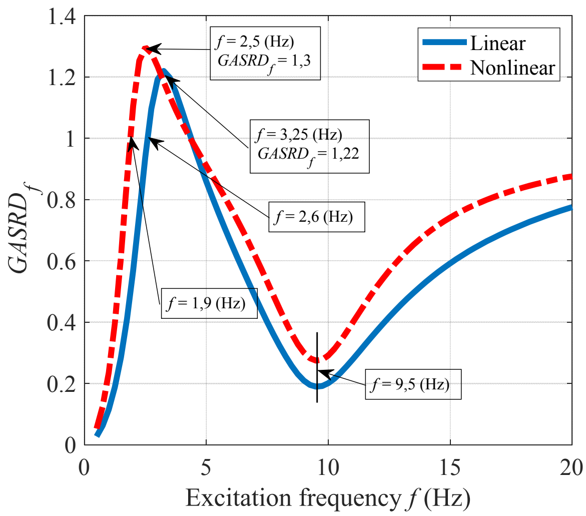

Figure 30. Gain response of the seat suspension relative displacement in the frequency domain $GASRD_f$

6. CONCLUSIONS

The dynamic model of the bus driver's seat suspension system with nonlinear elastic and damping elements, considering the dynamic influence of the guiding mechanism, has been entirely built. Vibration simulation results of the nonlinear suspension system are compared with the simple linear suspension system, from which the following conclusions are presented:

* In the average working velocity of 48 (km/h), the a_w value of body parts in the linear case is over 30% larger than the nonlinear case, specifically 32% in the head, 40% in the pelvis, 33.5% in the upper torso and 35,5% in the lower torso. However, both cases showed a level of sensation in the range without any uncomfortable sensations. The seat suspension system's *SEAT* value (%) reaches 93,5% and 74,1% for the linear and nonlinear cases, respectively.

* The comfort level and health when considering body parts increase as vehicle speed increases in linear and nonlinear cases. When considering the same body part, the acceleration of the linear case according to ISO 2631:1-1997 standard is always more significant than the nonlinear one. Considering the same part, the average acceleration increase of all parts at each speed of the linear and nonlinear cases has a minimal difference of less than 5%. Considering the same vehicle speed, the average acceleration increase of the parts in the nonlinear case is 8% larger than the linear case.

* The vibration isolation ability of the seat susp\–ension system in the linear and nonlinear cases differs by nearly 19% when the *SEAT* value in the nonlinear and linear cases is 74% and 93%, respectively.

* Response values in the frequency domain, inclu–ding acceleration response, displacement response, and vibration isolation ability in the linear case, have extreme response values greater than the nonlinear case by 1,6, 1,14, and 1,16 times, respectively. In the frequency range from 2,5 – 8,5 (Hz), the response value in the nonlinear case is always smaller than the linear case and vice versa when outside this frequency range.

ACKNOWLEDGEMENT

We acknowledge Ho Chi Minh City University of Technology (HCMUT), VNU-HCM for supporting this study.

REFERENCES

[1] M.J. Griffin, *Handbook of Human Vibration*, Elsevier Academic Press, London, 1996

[2] International Organization for Standardization (1997) ISO 2631-1: 1997, Mechanical Vibration and Shock - Evaluation of Human Exposure to Whole-body Vibration. Part 1: General Require-ments, Geneva, ISO

[3] Chia Wei, Susan G. Gerberich, Andrew D. Ryan, Bruce H. Alexander, Timothy R. Church, Michael Manser, *Risk factors for unintentional occupational injury among urban transit bus drivers: a cohort longitudinal study*, Annals of Epidemiology, vol. 17, pp. 763-770, 2017

[4] D. Karnopp, M. J. Crosby, R. A. Harwood, Vibration Control Using Semi-Active Force Generators, Journal of Engineering for Industry, pp. 619 – 626, 1974

[5] Reza N. Jazar. *Vehicle Dynamics: Theory and Application*. USA: Springer, 2008

[6] A. Heidarian and X. Quang, *Review on Seat Suspension System Technology Development*, *Applied Sciences*. vol. 9, 2019

[7] I. Maciejewski, L. Meyer and T. Krzyzynski. “Modelling and multi-criteria optimisation of passive seat suspension vibro-isolating properties,” *Journal of Sound and Vibration*. vol. 324, pp. 520-538, 2009

[8] S S Sun, D H Ning, J Yang, H Du, S W Zhang, and W H Li, A seat suspension with a rotary magnetorheological damper for heavy duty vehicles, *Smart Materials and Structures*, vol. 25, pp. 1-10, 2016

[9] I. Maciejewski, L. Meyer and T. Krzyzynski. “The vibration damping effectiveness of an active seat suspension system and its robustness to varying mass loading,” *Journal of Sound and Vibration*. vol. 329, pp. 3898-3914, 2010

[10] R. P. Blood, J.D. Ploger, M.G. Yost, R.P. Ching, P.W. Johnson, Whole body vibration exposures in metropolitan bus drivers: A comparison of three seats, *Journal of Sound and Vibration*. vol. 329, pp. 109-120, 2010

[11] S. Aisyah Adam and Nawal A. Abdul Jalil, Vertical Suspension Seat Transmissibility and SEAT Values for Seated Person Exposed to Whole-body Vibration in Agricultural Tractor Preliminary Study, *Engineering Physics International Conference, EPIC 2016*, vol. 170, pp. 435 – 442, 2017

[12] Ornwipa Thamsuwan, Ryan P. Blood, Randal P. Ching, Linda Boyle, Peter W. Johnson, Whole body vibration exposures in bus drivers: A comparison between a high-floor coach and a low-floor city bus, International Journal of Industrial Ergonomics, Elsevier, vol. 43, pp. 9-17, 2013

[13] Donghong Ning, Shuaishuai Sun, Haiping Du, Weihua Li, Wenxing Li, Control of a multiple-DOF vehicle seat suspension with roll and vertical vibration, *Journal of Sound and Vibration*. vol. 435, pp. 170-191, 2018

[14] Mahesh P. Nagarkar, Gahininath J. Vikhe Patil, Rahul N. Zaware Patil, Optimization of nonlinear quarter car suspension– seat–driver model, Journal of Advanced Research, vol. 7, pp. 991 – 1007, 2016

[15] Nagarkar, YJ Bhalerao, GJ Vikhe Patil, Zaware Patil, Multi-Objective Optimization of Nonlinear Quarter Car Suspension System – PID and LQR Control, 2nd International Conference on Materials Manufacturing and Design Engineering, vol. 20, pp. 420 – 427, 2018

[16] Haiping Du, Weihua Li, and Nong Zhang, Vibration Control of Vehicle Seat Integrating with Chassis Suspension and Driver Body Model, Advances in Structural Engineering, vol. 16, no. 1, pp. 1 – 9, 2013

[17] Haiping Du, Weihua Li, Nong Zhang, Integrated Seat and Suspension Control for a Quarter Car With Driver Model, IEEE Transactions on Vehicular Technology, vol. 61, no. 9, pp. 3893 – 3908, 2012

[18] Haiping Du, Semi-active control of an integrated full-car suspension with seat suspension and driver body model using ER dampers, Int. J. Vehicle Design, vol. 63, no. 2/3, pp. 159 – 184, 2013

[19] Giovani Gaiardo Fossati, Letı´cia Fleck Fadel Miguel, Walter Jesus Paucar Casas, Multi-objective optimization of the suspension system parameters of a full vehicle model, 2018

[20] Gavriloski, V., J. Jovanova, G. Tasevski, M. Đidrov, Development of a new air spring dynamic model, FME Transactions, 42, pp. 305-310, 2014

[21] Guida, D., Pappalardo, C.: A New Control Algo–rithm for Active Suspension Systems Featuring Hysteresis, FME Transactions, 41 pp. 285-290, 2013.

[22] Huu Nhan Tran, Ngoc Dai Pham, An investigation of the Wenda GI.34 bus driver seat based on the whole-body vibration exposure level, International Journal of Vehicle Noise and Vibration, vol. 19, no. 3/4, 2023

[23] International Organization for Standardization (ISO). “Mechanical vibration – Road surface profiles – Reporting of measured data.” Swit–zerland. Standard No. ISO 8608. ISO, 2016

[24] Wael Abbas, Ossama B. Abouelatta, Magdi El-Azab, Mamdouh Elsaidy, Adel A. Megahed, Optimization of Biodynamic Seated Human Models Using Genetic Algorithms, Engineering, vol. 2, pp. 710 – 719, 2010

[25] SaeedBadran, Ashraf Salah, Wael Abbas, Ossama B. Abouelatta, Design of Optimal Linear Suspen–sion for Quarter Car with Human Model using Ge–netic Algorithms, The Research Bulletin of Jordan ACM, vol. 2, no. 2, pp. 42 – 51, 2012

[26] European Directive 2002/44/EC (2002) of the European Parliament and of the Council of 25 June 2002 on the Minimum Health and Safety Requi–rements Regarding Exposure of Workers to the Risks Arising from the Physical Agents (Vibration), 2002. European Parliament

NOMENCLATURE

m_{se} = 35 (kg)	Mass of seat frame and cushion
m_p = 38 (kg)	Mass of pelvis
m_{lt} = 7,5 (kg)	Mass of lower torso
m_{ut} = 15 (kg)	Mass of upper torso
m_h = 4,17 (kg)	Mass of head
k_{se} (N/m)	Air spring’s stiffness
k_d = 58400 (N/m)	Cushion’s stiffness
k_{plt} = 20000 (N/m)	Stiffness between pelvis and lower torso
k_{put} = 144000 (N/m)	Stiffness between pelvis and upper torso
k_{lut} = 10000 (N/m)	Stiffness between upper torso and lower torso
k_{hut} = 166990 (N/m)	Stiffness between head and upper torso
c_{se} (Ns/m)	Damper’s damping coefficient
c_d = 217 (Ns/m)	Cushion’s damping coefficient
c_{plt} = 330 (Ns/m)	Damping coefficient between pelvis and lower torso
c_{put} = 909 (Ns/m)	Damping coefficient between pelvis and upper torso
c_{lut} = 200 (Ns/m)	Damping coefficient between upper torso and lower torso
c_{hut} = 310 (Ns/m)	Damping coefficient between head and upper torso
y_{se}, y_p, y_{lt}, y_{ut}, y_h (m)	Displacement of seat frame, pelvis, lower torso, upper torso, head
$\dot{y}_{se}, \dot{y}_p, \dot{y}_{lt}, \dot{y}_{ut}, \dot{y}_h$ (m/s)	Velocity of seat frame, pelvis, lower torso, upper torso, head
$\ddot{y}_{se}, \ddot{y}_p, \ddot{y}_{lt}, \ddot{y}_{ut}, \ddot{y}_h$ (m/s^2)	Acceleration of seat frame, pelvis, lower torso, upper torso, head
$y(t)$ (m)	Vehicle’s floor excitation

g = 9,81 (m/s^2)	Gravitational acceleration
μ = 0,08	Friction coefficient between sliders and sliding rails
$l = AC$ = 0,36 (m)	Guiding swing length

ПОРЕЂЕЊЕ ПОНАШАЊА ВИБРАЦИЈА ЛИНЕАРНОГ И НЕЛИНЕАРНОГ СИСТЕМА ВЕШАЊА СЕДИШТА ВОЗАЧА АУТОБУСА КОРИСТЕЋИ МОДЕЛ 5ДОФ

Ф.Н. Даи

Вибрације вешања возачевог седишта се анализирају коришћењем 5ДОФ модела. Систем вешања седишта укључује ваздушну опругу и хидраулички амортизер који има нелинеарно понашање одређено експериментално. Случајна побуда ир(т) је симулирана са стандардом ИСО 8608 кроз убрзање вибрација пода добијено помоћу уређаја ВМ31. Радни параметри укључују способ–ност изолације вибрација СЕАТ (%), ниво удоб–ности ав (м/с^2) (ISO 2631:1-1997) и утицај вибрација на здравље А(8) (2002/44/ЕС). При просечној брзини од 48 (км/х), вредности ав делова тела у линеарном случају су веће него у нелинеарном случају, тачно 32%, 40%, 33,5% и 35,5% у глави, карлици, горњем делу трупа и доњем делу трупа, респективно. СЕАТ вредност достиже 93,5% и 74,1% за линеарне и нелинеарне случајеве, респективно.